Formulation and numerical benchmark of improved magneto fluid-dynamics boundary conditions for 3D nonlinear MHD code SPECYL

L. Spinicci[1,2], D. Bonfiglio[1,3], S. Cappello[1,3], M. Veranda[1,3], L. Chacón[4]

[1] *Consorzio RFX, Euratom-Enea Association, Padova, Italy*

[2] *University of Padova, Padova, Italy,* [3] *ISTP, CNR, Milano-Padova-Bari, Italy*

[4] *Los Alamos National Laboratory, Los Alamos, USA*

Introduction: 3D nonlinear MHD code SpeCyl [1] is a spectral tool, operating in zero-β approximation and in cylindrical geometry to advance in time the magnetic field and the plasma flow. The traditional formulation of its boundary conditions (BCs), here dubbed SpeCyl.1, would see the plasma as if in direct contact with an ideal wall. However, a recent reformulation [2] introduced a rigid thin shell at the outer plasma radius and a tunable-width vacuum region between such shell and the ideal wall.

With a suitable choice of parameters, the resistive shell can be made transparent to the magnetic field, so to simulate a free-interface between plasma and vacuum. Numerical benchmark performed in this regime against current-driven linear MHD instabilities found good agreement concerning the internal modes, yet quantitatively poor for external MHD modes [3], motivating a reformulation of fluid boundary conditions, as well.

In this paper, we present the resulting set of BCs, here referred to as SpeCyl.2, a generalization to finite flow at plasma edge of the already present thin shell-like modelling of magnetic plasma-vacuum interface [2]. We include a mutual-benchmark between our new, self-consistent formulation SpeCyl.2 and another MHD nonlinear simulations code, Pixie3D [4], with analogous physical assumptions at plasma edge. This extends the nonlinear benchmark, already performed between the two codes [5] and verifies SpeCyl.2. We also provide numerical benchmarks, mainly against some well known results of the theory of linear MHD instabilities [6, 7].

SpeCyl.2 BCs feature the interface as thin, resistive shell [2], also allowing finite radial and tangent flow. On the top of an axisymmetric ohmic pinch equilibrium, as in [8], magnetic radial field modes $m,n \neq 0$ are assumed to be continuous across the shell. The cylindrical Poisson's problem is solved analytically in the vacuum region between the outer ideal wall and the resistive interface, to determine also azimuthal $B^{(m,n)}_{\theta,\mathrm{vac}}$ and axial $B^{(m,n)}_{z,\mathrm{vac}}$ magnetic components at interface, $r = a$, in terms of modified Bessel's functions. These values are used in the BCs

for their in-plasma counterparts, $B_\theta^{(m,n)}$ and $B_z^{(m,n)}$, enforcing tangent electric field continuity between the plasma and the shell, at $r = a$:

$$B_\theta^{(m,n)} \quad \text{from} \quad \frac{\eta_{\rm pl}}{\mu_0}\left[\frac{1}{a}\frac{\mathrm{d}}{\mathrm{d}r}\left(rB_\theta^{(m,n)}\right) - \frac{im}{a}B_r^{(m,n)}\right] - \left(v_r B_\theta - v_\theta B_r\right)^{(m,n)} = \frac{a}{\tau_w}\left[B_{\theta,\,\rm vac}^{(m,n)} - B_\theta^{(m,n)}\right] \tag{1}$$

$$B_z^{(m,n)} \quad \text{from} \quad \frac{\eta_{\rm pl}}{\mu_0}\left[\frac{in}{R}B_r^{(m,n)} - \frac{\mathrm{d}}{\mathrm{d}r}B_z^{(m,n)}\right] - \left(v_z B_r - v_r B_z\right)^{(m,n)} = -\frac{a}{\tau_w}\left[B_{z,\,\rm vac}^{(m,n)} - B_z^{(m,n)}\right] \tag{2}$$

where $\eta_{\rm pl}$ is plasma resistivity, R is the major radius, v and B are the flow and magnetic field, respectively. In both equations, the lhs represents the plasma electric field at edge, via the resistive Ohm's law, and the rhs is the electric field on the rigid shell, sustaining azimuthal and axial field jumps through eddy currents that plummet on the resistive timescale τ_w, given as an input. Permeability to finite edge flow is given by the turbulent $\mathbf{v}\times\mathbf{B}$ terms in round brackets, which are in fact convolutions over the full spectrum of the simulation.

The BCs for radial magnetic modes enforces Faraday's law and $\mathrm{div}\,\mathbf{B} = 0$ and read

$$B_r^{(m,n)} \quad \text{from} \quad \frac{\partial}{\partial t}B_r^{(m,n)} = \frac{1}{\tau_w}\left[\frac{\mathrm{d}}{\mathrm{d}r}\left(rB_{r,\,\rm vac}^{(m,n)}\right) - \frac{\mathrm{d}}{\mathrm{d}r}\left(rB_r^{(m,n)}\right)\right] \tag{3}$$

the derivative jump at rhs being sustained by eddy currents, shrinking on the wall time τ_w.

Finally, the BCs for the radial flow enforce the ideal Ohm's law, as an $\mathbf{E}\times\mathbf{B}$ drift, as in [8]:

$$v_r^{(m,n)} \quad \text{from} \quad \left(|B|^2 v_r\right)^{(m,n)} = \left(E_\theta B_z - E_z B_\theta\right)^{(m,n)} \tag{4}$$

whereas SpeCyl.1 only considered axisymmetric radial flow $v_r^{(0,0)} \neq 0$. Tangential components can be either set to 0 (no-slip) or fixed with a von Neumann like constraint (no-stress).

Mutual benchmark with Pixie3D here extends what already successfully done with SpeCyl.1, in [5], and serves to verify SpeCyl.2.

Figure 1 complements fig. 10 of [5] by comparing SpeCyl.2's new outcomes to SpeCyl.1's and Pixie3D's. This is a 2D case study of externally near-axis resonating $1/8$ kink in reversed-field pinch (RFP) geometry, with an ideal wall at $r = a$ and no-slip conditions on $\mathbf{v}$ (only the outermost 30% radial span is pictured). Ideal wall BCs coincide with setting the rhs of eqs. 1-3 to null (no field-jumps), so that the tangent electric field modes vanish on its surface (leftmost panel), whereas $E_z^{(0,0)} \neq 0$ to sustain equilibrium current density. In turn, this

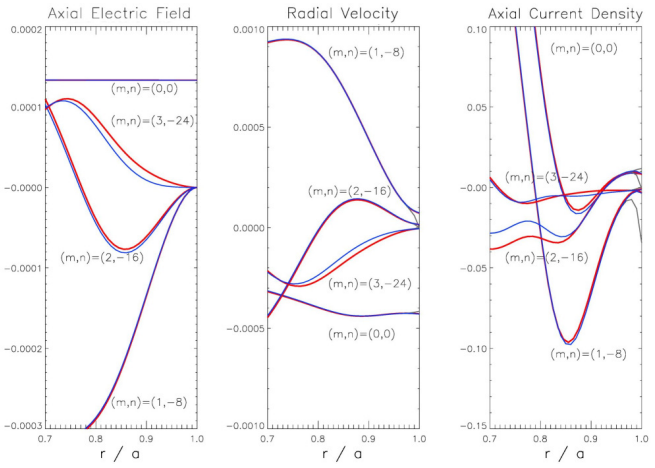

Figure 1: *Near-edge comparison of SpeCyl.1 (grey), SpeCyl.2 (blue) and Pixie3D (red) in RFP geometry.*

generates a mostly axisymmetric inwards *pinch* radial flow, via eq. 4 (see central panel): non-axisymmetric modes were completely missed by SpeCyl.1 and fall now in perfect agreement with Pixie3D, when using SpeCyl.2. A significant effect is observed on J_z modes (see last panel) since resistive Ohm's law with $E_z^{(m,n)} = 0$ sets them proportional to the $\mathbf{v} \times \mathbf{B}$ product, whose convolution is incomplete in SpeCyl.1, yielding unphysical edge-current spykes. As for the magnetic part of the BCs, fig. 2 shows the matching between SpeCyl's simulation radial field and the analytical solution of Poisson's problem in vacuum region, for the same RFP set-up, but with a second ideal conductor at $r/a = 10$. As long as the wall time τ_w is much longer than the simulation duration, almost no diffusion takes place. Instead, as time-scales get comparable, the slope imbalance flattens, according to eq. 3. As expected, SpeCyl.1 corresponds to the limit case for $\tau_w \to \infty$.

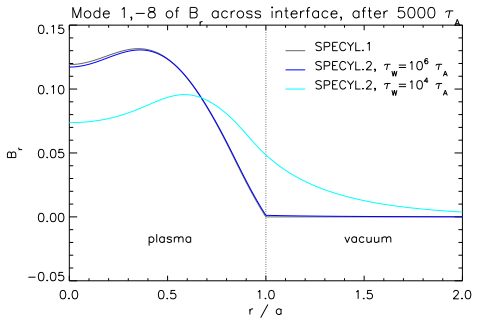

Figure 2: *SpeCyl.2* $B_r^{(1,-8)}$ *and analytical vacuum field, with ideal wall at* $r = 10a$. *SpeCyl.1 is recovered as* $\tau_W \to \infty$.

Benchmark against linear MHD in tokamak geometry has been performed extensively, especially against the external kink instability, where the edge flow plays a key role. We focus here on the specific case of $m = 2$ mode in large aspect-ratio (where zero-β approximation holds) and on a flat axial-current "Shafranov equilibrium" [7].

Linear model predictions can be achieved via the energy principle, that sets a variational problem to find the most favourable plasma-shape relaxation displacement $\xi = \sum_{m,n} \xi^{(m,n)}(r) \cdot \exp[im\theta + inz/R + i\omega t]$, with

$$\omega^2 = -\frac{W[\xi]}{\int_V \frac{\rho}{2}|\xi|^2 \mathrm{d}V}; \qquad W[\xi] = -\frac{1}{2}\int_V \mathbf{J} \times \mathbf{B} \cdot \xi \, \mathrm{d}V \tag{5}$$

the functional $W[\xi]$ being the (pressureless) work done by the plasma relaxation and $V = V_{\mathrm{pl}} + V_{\mathrm{vac}}$ the volume of the entire system. The variational principle reads $\delta W \equiv W[\xi + \delta\xi] - W[\xi] = 0$ for small $\delta\xi$, yielding an Euler's differential equation for ξ that solely depends on equilibrium current distribution and can be solved numerically. Substitution in eq 5 yields the growth-rate $\gamma = \mathtt{Im}\{\omega\}$, either positive (if unstable) or null.

Figure 3 illustrates SpeCyl.2 benchmark against Shafranov's model: we run 2D simulations with modes $m/n = 2/1$ and $4/2$ plus equilibrium, inverse aspect-ratio $\varepsilon = 0.05$, $\tau_w \sim \tau_A$, with uniform viscosity $\nu = 10^{-8}$ and no-stress BCs on $\mathbf{v}_{\|}$. Resistivity profile keeps almost flat onto $\eta(0) = 10^{-5}$, up to $r_{\mathrm{plasma}} = 0.9 \cdot a$, where it rapidly inflates to $100 \times \eta(0)$. Accordingly, plasma density ρ keeps uniform inside r_{plasma}, shrinking by a factor 10^4 outside it. Hence, we get a $\left[\rho, J_z^{(0,0)}\right] \approx const$ plasma region in $0 \le r \le r_{\mathrm{plasma}}$ and a narrow pseudo-vacuum layer. This

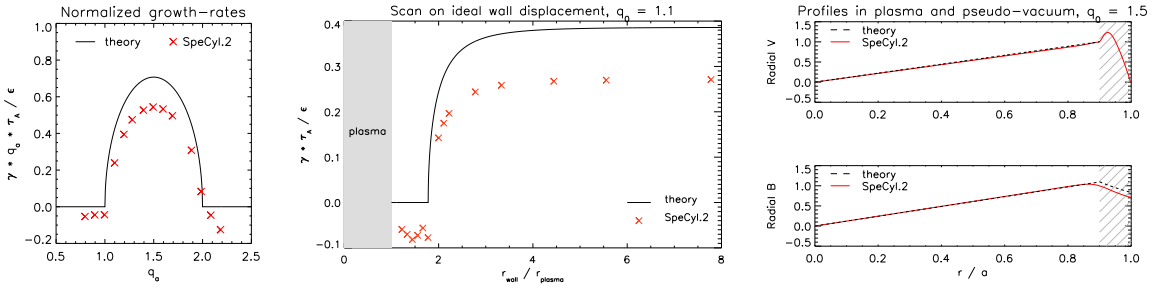

Figure 3: *Growth-rates and profiles of mode* $(2,-1)$ *external kink in the tokamak.*

approach is followed in several numeric codes, *e.g.* JOREK [9].

The first panel shows the growth rate dependence on the safety factor at edge: SpeCyl.2 underestimates its absolute value, but reliably predicts the instability margins, $1 < q_0 < 2$. Negative growth-rates outside this domain seemingly indicate coalescence of a stable ideal kink and a (numeric or visco-resistive) dissipative process. The central panel highlights the stabilizing effect of a closely-fitting superconductor: once more, the qualitative behaviour seems correct, with optimal matching of the critical wall distance at which the mode quenches. Quantitative results well agree with the analogous benchmark performed with JOREK [9]. Finally, very good agreement is found on profiles of both $v_r^{(m,n)}$ and $B_r^{(m,n)}$ in the meaningful plasma region, $r \leq 0.9 \cdot a$.

Conclusions SpeCyl.2 allows now a fully self-consistent resistive shell like interface and finite edge flow. Preliminary agreement on RFP geometry has been found with an independent simulations tool as Pixie3D, extending previous results and verifying both implementations. Also, qualitative and quantitative agreement with the theory of external kinks in tokamak geometry motivates further testing and research. Further verification is currently being sought via a benchmark against Pixie3D on $m = 1$ fundamental Kruskal-Shafranov limit.

Acknowledgments: This work has been carried out within the framework of the EUROfusion Consortium, funded by the European Union (EU) via the Euratom Research and Training Programme (Grant Agreement No 101052200 — EUROfusion). Views and opinions expressed are however those of the authors only and do not necessarily reflect those of the EU or the European Commission (EC). Neither the EU nor the EC can be held responsible for them.

References

[1] S. Cappello, et al., Am. Inst. of Phys. 978-0-7354-0600 (2008)

[2] L. Marrelli et al., Nucl. Fus. **59** 076027 (2019)

[3] L. Spinicci et al., 19th EFTC contributions, #55 (2021)

[4] L. Chacón, Phys. of Pl. **15**, 5, 056103 (2008)

[5] D. Bonfiglio et al., Phys. of Pl. **17**, 8, 082501 (2010)

[6] J.A. Wesson, Nucl. Fus. **18**, 1, 87 (1978)

[7] J.P. Freidberg, "Ideal MHD", chap. 8-11, Camb. Univ. Press (2014)

[8] G. L. Delzanno, L. Chacón, J. Finn, Phys. of Pl. **15**, 122102 (2008)

[9] R. Mc Adams, PhD thesis, chap. 5, Univ. of York (2014). `https://etheses.whiterose.ac.uk/7723/`